

Optical Anisotropy in a Quantum-Well-Wire Array with Two-Dimensional Quantum Confinement

M. Tsuchiya, J. M. Gaines, R. H. Yan, R. J. Simes, P. Ö. Holtz, L. A. Coldren, and P. M. Petroff

*Department of Electrical and Computer Engineering and Materials Department,
University of California, Santa Barbara, California 93106*

(Received 20 June 1988)

A photoluminescence study of an (AlGa)As-GaAs quantum-well-wire array directly grown by molecular-beam epitaxy on a tilted substrate is described. A strong anisotropy was observed in the ratio of the electron-light-hole-exciton peak intensity to the electron-heavy-hole-exciton peak intensity. A theory incorporating the optical selection rule for two-dimensional quantum confinement is found to agree very well with the measured data. These results constitute the first evidence of two-dimensional *quantum* confinement in artificial wire structures having cross-sectional dimensions in the nanometer range.

PACS numbers: 78.65.Fa, 73.20.Dx, 78.55.Cr

Low-dimensional structures^{1,2} having quantum confinement (QC) of two or three dimensions such as quantum-well wires (QWW's) and quantum-well boxes (QWB's) have in the last few years attracted much attention not only for their potential in uncovering new phenomena in solid-state physics but also for their potential device applications. Extremely high electron mobility in QWW's¹ and high performance of QWW or QWB lasers³ and modulators⁴ are expected from theoretical predictions. Recent experiments in QWB resonant-tunneling devices⁵ have in fact claimed to demonstrate new structures that are attributed to a zero-dimensional system. Transport measurements in narrow wires have also demonstrated a complete quenching of the Hall effect⁶ associated with the one-dimensional quantum transport.

Most of these low-dimensional structures have been made by fine lithographical methods⁷ such as electron-beam lithography, focused-ion-beam implantation, impurity-induced interdiffusion, etc. However, the lateral dimensions in such structures have been much larger than the vertical dimensions and still in the submicron-meter range, leading to relatively small separations of subband energies. In most cases, the width broadening of energy levels have been larger than the energy separations, and these lithographical techniques seem to have intrinsic difficulties. However, a new approach⁸ to control the nucleation and growth kinetics available with molecular-beam epitaxy (MBE) on vicinal substrates has made possible the direct growth of QWW superlattices. Recently, a two-dimensional band-gap modulation of tilted superlattices (TSL) was successfully demonstrated by use of MBE⁹ and organometallic-vapor-phase epitaxy.¹⁰ In those structures, the lateral dimensions are in the low-nanometer range. It is currently the only technique to make QWW arrays with these dimensions, and initial measurements, as reported here, suggest that it may be an extremely powerful technique for QWW device structures.

In this paper, we report a photoluminescence (PL) study on a QWW array prepared directly by MBE, and the observation of a strong optical anisotropy in PL excitation (PLE) spectra: The ratio of electron-light-hole-exciton peak intensity (I_{lelh}) to electron-heavy-hole-exciton peak intensity (I_{lehh}) depends strongly on the polarization orientation of the incident light with respect to the QWW direction. Relative matrix elements of optical transitions were also calculated by taking the optical selection rules into account. A good agreement of the measured data was found with our theoretical prediction, and we believe it is the first clear evidence of two-dimensional *quantum* confinement (2D QC) in artificial QWW's which have sizes in the low-nanometer range.

We designed a QWW array¹¹ shown in Fig. 1(a) on a vicinal (001) semi-insulating GaAs substrate tilted 2° toward [110]; the average step size is 8 nm. In this structure, carriers are expected to be pushed from the TSL region to the GaAs layer and be confined laterally by the potential variation of the TSL (~4 nm GaAs per 4 nm AlAs).^{11,12} Quantum-level broadening due to the step-size fluctuation is expected to be smaller because of the relatively weak lateral confinement as compared to QWW's with fully surrounding AlAs barriers. A single layer of the above QWW array was grown by MBE as follows. First, a GaAs buffer layer of 300 nm was grown at 400°C to make surface steps uniform; it was followed by 600°C growth of a 50-nm Al_{0.2}Ga_{0.8}As barrier, 5 nm of GaAs, TSL layer of 5 nm, and a 50-nm Al_{0.2}Ga_{0.8}As barrier. All layers were deposited by alternate beam growth⁸ (of Ga and/or Al) and As to enhance the migration of Ga and Al atoms on the wafer surface. The TSL was prepared by growing superlattices (GaAs)_m(AlAs)_n with the fraction of monolayers $m/n \sim 0.5$. Finally, a 10-nm cap GaAs layer was deposited. As seen in Fig. 1(b), the TSL was clearly observed in the transmission-electron-microscopy cross section of the sample. The contrast in this micrograph reflects the Al content (chemical contrast) of the various regions. The darker

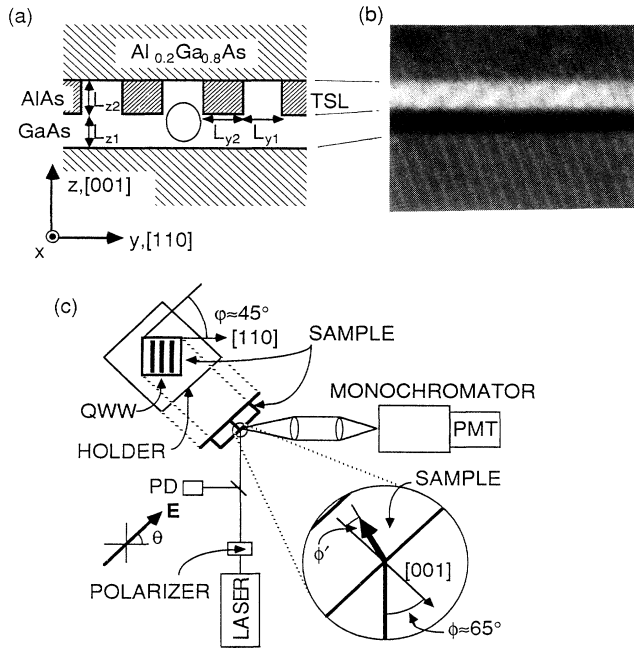


FIG. 1. (a) Schematic illustration of the QWW array in the present work. It was designed to have $L_{z1}=L_{z2}=5$ nm, $L_{y1}=L_{y2}=4$ nm. (b) Transmission-electron-microscopy cross section of the QWW sample taken in the dark-field mode with a forbidden reflection $\{200\}$ for the GaAs structure. The dark region corresponds to the 5-nm GaAs layer and the lighter region to the structure with the higher Al content. (c) The schematic of the PL and PLE measurement. The sample was mounted on a holder in the liquid-He cryostat with the $[110]$ axis tilted by φ with respect to the horizon. The (001) plane was set at an angle ϕ with respect to the laser beam. The excitation light of the dye laser was polarized at an angle θ by a Glan-Thompson prism with respect to the horizon. θ was varied from 30° to 165° . ϕ was nearly 65° , and φ was 45° .

region corresponds to the 5-nm GaAs layer and the lighter region to the structure with the higher Al content.

The apparatus shown in Fig. 1(c) was used for the PL measurement. Polarized light was selected by a Glan-Thompson prism from the dye laser having nearly vertical polarization. A portion of the laser beam through the polarizer was divided, detected by a photodetector, and used as a reference to normalize the PL intensity. The sample was mounted on a flat holder with the $[110]$ axis tilted by φ ($\sim 45^\circ$) with respect to the horizon. Although the (001) plane was set at an angle ϕ ($\sim 65^\circ$) with respect to the incident laser beam, the path of the refracted beam in the sample is nearly normal to the surface plane ($\phi' \sim 15^\circ$) due to the large index of the wafer. Hence, the electric field vector can be rotated nearly in the (001) plane. The PL signal was detected by a photomultiplier tube (PMT) through a grating monochromator.

First, we measured PL of a conventional quantum well

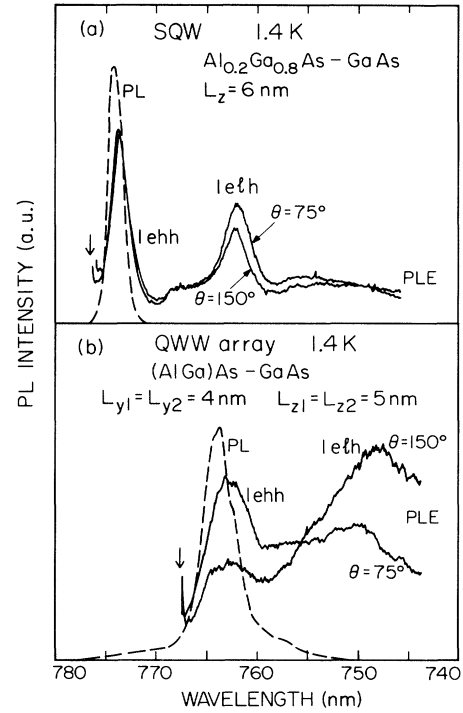


FIG. 2. PL spectra (dashed lines) and PLE (solid lines) of (a) a single quantum well (SQW) and (b) a quantum-well-wire (QWW) array, respectively. The parameter θ is the polarization angle of the excitation laser light with respect to the horizon. Arrows show the detection wavelengths.

(QW) at 1.4 K. The QW consists of a 6-nm GaAs well with $\text{Al}_{0.2}\text{Ga}_{0.8}\text{As}$ barriers. A sharp PL peak was observed at 774 nm; its full width at half maximum was 3.7 meV. PLE spectra were measured as a function of the polarization angle θ of the incident laser light. Although well-resolved exciton peaks were observed in the PLE spectra as shown in Fig. 2(a), no polarization dependence was found ($I_{1elh}/I_{1ehh} \sim 0.4$).

Then, the PL spectra for the QWW sample were measured at 1.4 K. As seen in Fig. 2(b), a prominent and fairly sharp PL peak was observed at 764 nm; its full width at half maximum was 7.7 meV. The slope at lower energy is steeper than at higher energy, and a tail structure was also found at the higher-energy side, which indicates the broadening of the ground quantum level due to the fluctuations in the lateral widths of the QWW's. PLE spectra were also measured as a function of θ . Typical PLE spectra at $\theta=75^\circ$ and at $\theta=150^\circ$ (which correspond to nearly orthogonal polarizations in the sample) are shown in Fig. 2(b). Clear electron-heavy-hole-exciton (1ehh) and electron-light-hole-exciton peaks (1elh) were observed. Since the energy separation of subbands is expected to be much larger than the 1ehh-1elh separation in this structure, the broadening of PLE peaks is also due to the fluctuation of

the QWW sizes. Note in Fig. 2(b) the strong anisotropy of the PLE spectra for the 1elh and 1elh signals. For the light polarized with its electric field vector nearly parallel to the QWW's ($\theta=75^\circ$), the 1elh peak is more intense than the 1elh peak ($I_{1elh}/I_{1elh} \sim 0.4$); whereas the I_{1elh} was drastically enhanced when the incident light was polarized nearly perpendicular to the QWW's ($\theta=150^\circ$, $I_{1elh}/I_{1elh} \sim 1.8$). The variation of I_{1elh}/I_{1elh} with θ is plotted in Fig. 3.

To clarify the origin of the polarization dependence, we have calculated the momentum matrix elements M of the QWW's. As is well known, the intensity of an optical transition, i.e., absorption, is proportional to $|M|^2$ of the materials. After Kane's matrix elements¹³ derived by the k - p theory, M are functions of the directions of both vector potential \mathbf{A} of the incident photon and electron wave vector $\mathbf{k}=(k_x, k_y, k_z)$. The momentum matrix elements of the excitons are given by the integration over \mathbf{k} , the product of $M(\mathbf{k}, \mathbf{A})$, and the envelope of the exciton wave function. In the QWW's, k_y and k_z are discrete because of QC, and $1/k_y$ and $1/k_z$ are fixed in the several-nanometer range while k_x is continuous because of the lack of QC. Hence, anisotropy of M with respect to the direction of \mathbf{A} is caused by the terms including both \mathbf{k} and \mathbf{A} . In addition, M of the heavy holes depends on the direction of \mathbf{A} differently from that of the light holes. Hence, the optical anisotropy is expected in the ratio of I_{1elh}/I_{1elh} in absorption spectra when the electric vector of the incident light is rotated in the plane

of the QWW array. Since the PL intensity is proportional to the number of photons absorbed, the same anisotropy is expected to appear also in the PLE spectra.

With the assumption that the effective widths L_y^* and L_z^* of the QWW's are equal [Fig. 1(a)], the above consideration leads to a ratio of I_{1elh}/I_{1elh} given by the expression

$$\frac{I_{1elh}}{I_{1elh}} = \frac{\frac{1}{2} |E_p|^2 + \frac{5}{4} |E_n|^2}{\frac{3}{2} |E_p|^2 + \frac{3}{4} |E_n|^2} \quad (1)$$

Here, E_p and E_n are the electric field components parallel and normal to the QWW's, respectively, which were calculated by Fresnel's relation. The fractions in front of $|E_p|^2$ and $|E_n|^2$ show the relative strength of optical transitions of the 1elh exciton in the first parentheses and of the 1elh exciton in the second. In this first-order calculation, well-confined, one-dimensional excitons are assumed. It is also assumed that the dependence of M on k_x is negligible. Although the one-dimensional exciton wave function contains some components over k_x , the approximation will not give large errors.⁴ The ratio I_{1elh}/I_{1elh} and its polarization dependence thus calculated are plotted in Fig. 3. Here, it is assumed that $\phi=65^\circ$ and $\varphi=45^\circ$. Note the good agreement with the measured data, although there is some offset in θ , caused in setting the polarizer and the holder. Such agreement strongly indicates 2D QC in our QWW array. More detailed calculations show the existence of relatively strong lateral confinement in the QWW array, although some lateral wire-wire coupling is present, leading to more complicated anisotropy than given by Eq. (1). The calculation will be reported elsewhere. Discrepancies between measured data and the theory near $\theta=150^\circ$ are attributable to either the error in the determination of I_{1elh} in the spectra, or to anisotropy in L_y^* and L_z^* , since the ratio I_{1elh}/I_{1elh} at the light polarization along y direction increases when the ratio L_z^*/L_y^* increases.

In summary, we have observed for the first time a strong optical anisotropy due to two-dimensional quantum confinement in a QWW array directly deposited by MBE. The observed optical anisotropy was explained well by the theory of the relative optical transition strength. The data show that such QWW structures have great promise for use in novel optical devices.

The authors would like to thank Professor H. Kroemer, Professor J. L. Merz, Professor A. C. Gossard, J. H. English, and R. S. Geels for useful discussions and collaboration. This work was supported in part by the Innovative Science & Technology Directorate of the Strategic Defense Initiative Organization via ARO and ONR.

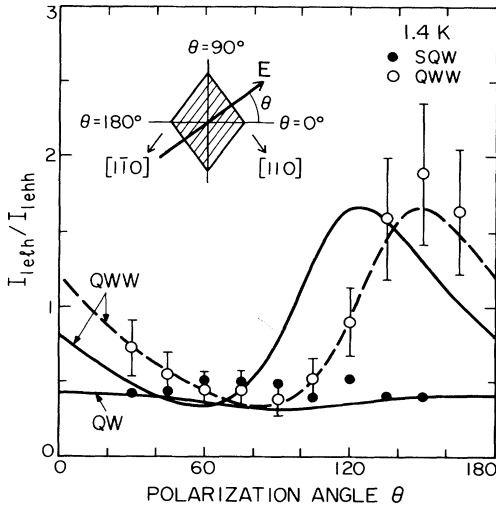


FIG. 3. The ratio of the area of PLE peak for electron-light-hole exciton (I_{1elh}) to that for electron-heavy-hole exciton (I_{1elh}) is plotted as a function of θ . Solid circles and open circles show the polarization dependence of the SQW and the QWW, respectively. Solid curves are theoretical calculations. The dashed line is shifted from the theoretical curve by an offset of $\Delta\theta=25^\circ$. Inset: Projection of the sample as seen by the polarized incident light.

¹H. Sakaki, Jpn. J. Appl. Phys. **19**, 94 (1980).

²P. M. Petroff, A. C. Gossard, R. A. Logan, and W. Wieg-

man, Appl. Phys. Lett. **41**, 635 (1982).

³Y. Arakawa and H. Sakaki, Appl. Phys. Lett. **40**, 939 (1982).

⁴I. Suemune and L. A. Coldren, IEEE J. Quantum Electron. **24**, 1178 (1988).

⁵M. A. Reed, J. N. Randall, R. J. Aggarwal, R. J. Matyi, T. M. Moore, and A. E. Wetsel, Phys. Rev. Lett. **60**, 535 (1988).

⁶M. L. Roukes, A. Scherer, S. J. Allen, Jr., H. G. Craighead, R. M. Ruthen, E. D. Beebe, and J. P. Harbison, Phys. Rev. Lett. **59**, 3011 (1987).

⁷See, for example, J. Cibert, P. M. Petroff, G. J. Dolan, S. J. Pearton, A. C. Gossard, and J. H. English, Appl. Phys. Lett. **49**, 1275 (1986).

⁸P. M. Petroff, A. C. Gossard, and W. Weigmann, Appl.

Phys. Lett. **45**, 620 (1984).

⁹J. M. Gaines, P. M. Petroff, H. Kroemer, R. J. Simes, R. S. Geels, and J. H. English, J. Vac. Sci. Technol. B **6**, 1378 (1988).

¹⁰T. Fukui and H. Saito, Appl. Phys. Lett. **50**, 824 (1987).

¹¹Such a structure was first discussed by Sakaki *et al.*, and its formation was previously attempted by Tanaka and Sakaki. See H. Sakaki, K. Wagatsuma, J. Hamasaki, and S. Saito, Thin Solid Films **36**, 497 (1976); M. Tanaka and H. Sakaki, in Proceedings of the Fifth Symposium on Alloy Semiconductor Physics and Electronics, Kyoto, Japan, 1988 (to be published).

¹²Y. C. Chang, L. L. Chang, and L. Esaki, Appl. Phys. Lett. **47**, 1324 (1985).

¹³E. O. Kane, J. Phys. Chem. Solids **1**, 249 (1957).

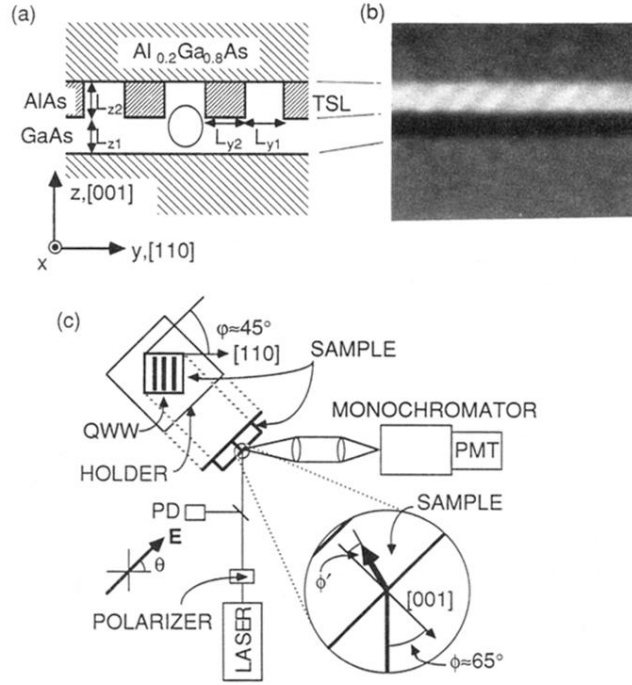


FIG. 1. (a) Schematic illustration of the QWW array in the present work. It was designed to have $L_{z1}=L_{z2}=5$ nm, $L_{y1}=L_{y2}=4$ nm. (b) Transmission-electron-microscopy cross section of the QWW sample taken in the dark-field mode with a forbidden reflection $\{200\}$ for the GaAs structure. The dark region corresponds to the 5-nm GaAs layer and the lighter region to the structure with the higher Al content. (c) The schematic of the PL and PLE measurement. The sample was mounted on a holder in the liquid-He cryostat with the $[110]$ axis tilted by ϕ with respect to the horizon. The (001) plane was set at an angle ϕ with respect to the laser beam. The excitation light of the dye laser was polarized at an angle θ by a Glan-Thompson prism with respect to the horizon. θ was varied from 30° to 165° . ϕ was nearly 65° , and φ was 45° .